

Synthesis, Characterization of Some Surfactants Based on Di-Oleamide and Evaluation of Their Efficiency as Corrosion Inhibitors for Oil Wells Tubing Steel under CO₂ and H₂S environment

M.A. Migahed¹, A.M. Al-Sabagh¹, E.S. Gad², F. Abd El-Hay², H. M. Abd EL-Bary²

¹Egyptian Petroleum Research Institute (EPRI), Nasr City, Cairo 11727, Egypt

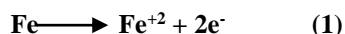
²Chemistry Department, Faculty of Science, Al-Azhar University, Cairo, Egypt

Abstract: Novel surfactants namely; *N,N'*-(((2-(2-hydroxyethoxy)ethyl)azanediyl)bis(ethane-2,1-diyl)bis(*N*-(2-(2-hydroxyethoxy)ethyl)oleamide) (I), *N*-(2-(2-hydroxyethoxy)ethyl)*N,N*-bis (2(*N*-(2-hydroxyethoxy)ethyl)oleamido)ethyl)propan-2-aminium bromide (II) and *N*-(2-(2-hydroxyethoxy)ethyl) -*N,N*-bis (2-(*N*-(2-(2-hydroxyethoxy)ethyl)oleamido)ethyl)-4-methylbenzenaminium bromide (III), were synthesized, characterized by using FTIR and ¹HNMR spectroscopic methods. Potentiodynamic polarization and electrochemical impedance spectroscopy (EIS) techniques were used to evaluate the performance of the synthesized surfactants as corrosion inhibitors for X-70 type tubing steel in deep oil wells formation water under CO₂ and H₂S environment at 25 °C. Polarization curves showed that by increasing the inhibitor concentration the corrosion current density was decreased, and the presence of inhibitor molecules affect on both cathodic and anodic Tafel lines, but the cathodic effect is more pronounced. Data obtained from EIS technique were analyzed to model the corrosion inhibition process through equivalent circuit (EC). Quantum chemical calculations based on ab initio method were performed on I, II and III. The molecular structural parameters, such as the frontier molecular orbital energy HOMO (highest occupied molecular orbital) and LUMO (lowest unoccupied molecular orbital), and the fraction of electrons (Δ*N*) transfer from inhibitor to carbon steel surface were calculated and discussed. Finally, the nature of the formed protective film was analysed by SEM and EDX techniques. The results showed that the selected surfactants have good efficiencies as corrosion inhibitors for tubing steel in deep oil wells formation water under CO₂ and H₂S environment.

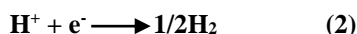
Keywords: Corrosion, Surfactants, EIS, Tafel,

1. Introduction

Corrosion process is an irreversible interfacial reaction of a material with its environment, resulting in the loss of material [1]. It plays an important role in the field of economics and safety. Carbon steel is a major construction material and is extensively used throughout petroleum industry from production to refinery [2]. The cost of replacing, repairing and maintaining steel pipelines resulting from corrosion process in oil field is extremely expensive and time-consuming [3-5]. Sweet and sour conditions in oil and gas wells are very corrosive environments caused by trace amounts of oxygen entering into a sour brine system, as well as the large amounts of CO₂ and H₂S present in deep oil well water (formation water). Both CO₂ and H₂S behave like weak acids. As such, they are able to provide oxidizing power and promote iron corrosion, establishing equilibrium between oxidation and reduction reactions:



The most common reduction reaction in de-aerated acid media is proton reduction:

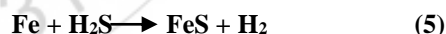


Carbon dioxide present in sweet wells forms a weak carbonic acid (H₂CO₃) solution in aqueous media which

attack the steel pipeline and forms iron carbonate (FeCO₃) with the evolution of H₂[6].



The corrosion reaction of iron with H₂S occurred mainly by a solid state reaction, via the global reaction scheme [7]:



Corrosion in the oil field appears as leak in tanks, casing, tubing, pipe line and other equipment. This process changes the base metal to another type of materials [8, 9]. It is well known that corrosion inhibitor is an additive with significantly ability to inhibit metal corrosion in the corrosive solution [10-12]. Carbon steel used in combination with corrosion inhibitors is, however, the favored alternative for such pipelines, on economic grounds, compared to the use of corrosion-resistant materials. These corrosion inhibitors are usually composed of organic, surface-active molecules which are believed to form self-assembled films that protect the steel surface against corrosion [13]. To be effective, an inhibitor must displace water from the metal surface, interact with anodic or cathodic reaction sites to retard the oxidation and reduction corrosion reaction, prevent transportation of water and corrosion active species on the surface [14]. Many efficient organic inhibitors have heteroatom and multiple bonds or aromatic rings in their structures. As a representative type of these organic inhibitors, quaternary ammonium salts

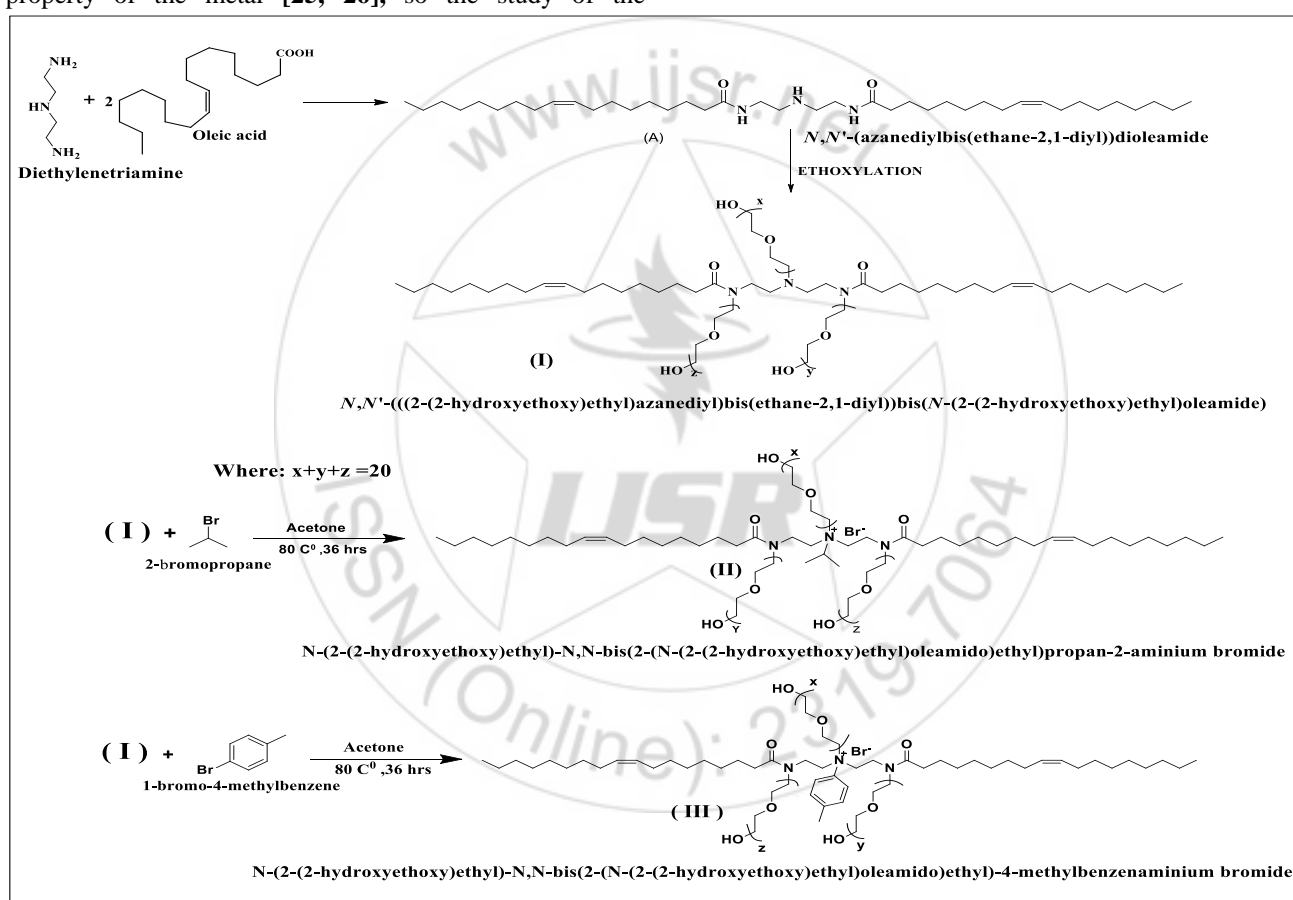
have been demonstrated, to be highly effective in corrosion inhibition for different aggressive media, in our lab and by other previous research [15–17]. Surfactants are special type of organic compounds and exhibit unique properties due to their amphiphilic molecule. This is the reason of their wide application in the field of inhibition of metals against corrosion. The surfactant inhibitor has many advantages such as high inhibition efficiency, low price, low toxicity and easy production [18–23]. The efficiency of the inhibition film depends on the inhibitor concentration and contact time with the metal surface. In fact, introducing of ethylene oxides into surfactant molecule (ethoxylation) increases the inhibitive effect of surfactant [24]. The presence of these groups increases the solubility of surfactant and hence the extent of its adsorption on the metal surface increases and consequently its inhibitive action improves. The adsorption of the surfactant on the metal surface can markedly change the corrosion resisting property of the metal [25, 26], so the study of the

relationship between the adsorption and corrosion inhibition is of great importance. Quantum chemical calculations have been proved to be a very powerful tool for studying the inhibition mechanism [27, 28]. The present study is aimed to synthesis one non-ionic and two cationic surfactants and evaluate their performance as corrosion inhibitors for carbon steel in oil wells formation water under CO₂ and H₂S environment. The choice of these compounds was based on molecular structure considerations that, these compounds contain hetero-atoms such as N and O, which induce greater adsorption of the inhibitor molecule onto the surface of carbon steel.

2. Experimental Method

2.1. Synthesis of nonionic surfactant (Base Compound)

Novel surfactants used in this study were synthesized as shown in Scheme 1.



Scheme (1): Illustrate the formation of surfactants.

This process was carried out in two steps as follow:

2.1.1. Formation of oleic acid diamide

A solution of oleic acid (0.04 mol) in xylene (100 ml) was added dropwise by syringe to a solution of diethylenetriamine (DETA) (2.06 g, 0.02 mol) in xylene (25 ml) under reflux. After addition was complete (1h), the reaction mixture was refluxed for 4 h. After removing the solvent, the residue was recrystallized to give (A) [29].

2.1.2. Synthesis of the ethoxylated compounds.

A high pressure stainless steel autoclave (parr model 4530, USA) of 1L capacity, 400 psi maximum pressure and 100 °C

maximum temperatures was utilized through ethoxylation reaction. (A) was charged into the reaction vessel with triethyl amine as a catalyst (0.3 wt %) and heated to 80 °C with continuous stirring while passing a stream of nitrogen gas through the system for 10 minutes to flush out air [30]. The nitrogen stream was then replaced by ethylene oxide, 20 units of ethylene oxide was introduced to the namely (A) through the inlet gas valve until the desired amount of ethylene oxide was introduced as shown in Scheme 1. At this stage, heating was stopped and the contents were cooled gradually to ambient temperature by means of the cooling coil connected to the reactor carrying cold water. After cooling, the obtained product was discharged, weighted and neutralized with HCl,

dissolved in isopropanol, then salted out with supersaturated NaCl solution. The organic layer was then separated and the isopropanol was distilled off. The ethoxylated product which named (I) obtained showed a brown viscous liquid appearance [31].

2.2. Synthesis of Cationic Surfactants.

Aliphatic cationic surfactants and aromatic cationic surfactants used in this study were synthesized as shown in **Schemes 1**.

A mixture of (I) and different alkyl bromides (Isopropyl Bromide or 4-Bromo-Toluene) using an excess of alkyl bromide (25%) and acetone as solvent was refluxed for 36 h. After rotary evaporation of the acetone, a high viscous liquid was obtained [32]. The resulting product was recrystallised to give the corresponding cationic surfactant which namely (II) for aliphatic cationic surfactants and namely (III) for aromatic cationic surfactants.

2.3. Chemical composition of the investigated carbon steel

Carbon steel specimens used in this investigation were cut from unused petroleum pipeline. The chemical composition of carbon steel alloy is listed in **Table 1**.

2.4. Test solution

The test solution for this work consists of Na_2S (0.006M), Na_2CO_3 (0.05M) and HCl (1%) dissolved in the deep oil well formation water naturally exists in the reservoir rocks before drilling. Most oil field water contains a variety of dissolved organic and inorganic compounds. The major elements usually present are sodium, calcium, magnesium, chloride, bicarbonate, and sulphate. The chemical composition of the oil wells formation water used in this investigation and its physical properties are shown in **Table 2**.

2.5 Inhibitor solutions

1000 ml stock solutions of the organic compound were prepared by dissolving (1 gm) of the solid material using de-ionized distilled water. Then the required concentrations (concentration ranged from 100 to 500 ppm) were prepared by dilution using test solution.

2.6. Measurement of surface tension

Equilibrium surface tension measurements were made at 25 °C using the Du Nouy ring method Tensiometer (Kruss Type 6) for different concentrations of the synthesized surfactants. All solutions were prepared in double distilled water with a surface tension equal 72 mN m⁻¹ at 25 °C.

2.7 Electrochemical measurements

The electrochemical measurements were carried out using Voltalab 80 (Tacussel-radiometer PG Z402). In this method, the working electrode was immersed in the test solution for 3h until the open circuit potential was reached. After that the working electrode was polarized in both cathodic and anodic directions. Standard ASTM glass electrochemical cell was used. Platinum electrode was used as auxiliary electrode. All potentials were measured against a SCE as reference electrode. Potentiodynamic polarization measurements were obtained by changing the electrode potential automatically from -950 to -350 mV vs. SCE with

a scan rate 2 mV s⁻¹ at 25 °C. Impedance spectra were obtained in the frequency range between 100 kHz and 50 mHz using 10 steps per frequency decade at open circuit potential after 3 hours of immersion time. AC signal with 20 mV amplitude peak to peak was used to perturb the system. EIS diagrams are given in Bode and Nyquist representations.

2.8 Scanning electron microscopy

The surface examination was carried out using scanning electron microscope (JEOL JSM-5410, Japan). The energy of the acceleration beam employed was 25 KV. All micrographs were taken at a magnification power (X 1000).

2.9 Energy dispersive analysis of X-rays (EDX)

EDX system attached with a JEOL JSM-5410 scanning electron microscope was used for elemental analysis or chemical characterization of the film formed on carbon steel surface before and after applying the synthesized inhibitor (III).

2.10 Quantum chemical study

The molecular structures of the investigated surfactants had been fully geometric optimize by ab initio method (3-21G** basis set) with Hyperchem 7.5, the following quantum chemical parameters calculated are the energy of the highest occupied molecular orbital (E_{HOMO} , eV), the energy of the lowest unoccupied molecular orbital (E_{LUMO} , eV), the energy gap ($\Delta E = E_{\text{HOMO}} - E_{\text{LUMO}}$, eV), the dipole moment (μ , Debye), log P (lipophilicity) and the number of transferred electrons (ΔN)

3. Results and discussion

3.1. Confirmation of chemical structure of the prepared inhibitors

The chemical structure of the prepared cationic surfactants was confirmed by the FTIR and ¹H NMR spectroscopy as shown in **Figs. 1, 2** respectively for compound III as representative sample. From the obtained spectra, it was found that the C–O band of the ethoxylated appeared at 1121 cm⁻¹. The main band denotes to N⁺ appeared at 1377 cm⁻¹. The C=O band for amide group appeared at 1657 cm⁻¹. The terminal –OH group of ethoxylated primary amine was found at 3286 cm⁻¹ as abroad band, C–H aliphatic at 2854–2925 cm⁻¹ and All the above chemical shifts confirm the cationic compound III was success, fully prepared as showed in Fig. (2). The chemical shifts for CH₃- group at (a) 0.81 for terminal CH₃- of oleic acid, (b) 2.46 for CH₃- of tolyl group. The chemical shifts for CH₂- group at (a) 3.96 of the CH₂-group in the first ethylene oxide unit attached to 3° N, (b) 3.55 of the CH₂- group of repeated ethylene oxide units, (c) 1.19 of the CH₂-group in the oleic acid, (d) 2.24 of the CH₂-group in adjacent to amide group and (e) 4.07 of the CH₂-group in the ethylene oxide unit attached to 4° N. The chemical shifts for CH- group at 5.28 ppm. 7.063–7.78(m, 4H, Ar-H). The above chemical shifts confirm that the cationic derivatives were successfully prepared. The data of ¹H NMR spectra confirmed the expected hydrogen proton distribution in the synthesized cationic surfactants.

3.2. Polarization measurements

Both anodic and cathodic polarization curves for carbon steel in the test solutions at different concentrations of compound III

as a representative sample are shown in **Fig 3**. It is clear that the presence of the inhibitors causes a markedly decrease in the corrosion rate as the values of corrosion current density (I_{corr}) decrease by increasing the inhibitor concentrations. Values of the corrosion current densities (I_{corr}), corrosion potential (E_{corr}), cathodic Tafel slope (β_c), and anodic Tafel slope (β_a) were calculated from the obtained polarization curve and are listed in **Table 3**. From these data, it is clear that the corrosion current decreases with the increase in the inhibitor concentration. The presence of the prepared surfactants does not remarkably shift the corrosion potential, while the anodic and cathodic Tafel slopes change with the increase in the inhibitor concentration. Therefore, the prepared surfactants can be classified as mixed-type inhibitors. The degree of surface coverage (θ) and the percentage inhibition efficiency ($\eta_p\%$) were calculated using the following equations [33]:

$$\theta = [1 - (i/i_0)] \quad (6)$$

$$\eta_p \% = [1 - (i/i_0)] \times 100 \quad (7)$$

where i_0 and i are the corrosion current densities in the absence and presence of the inhibitor, respectively. Values of the inhibition efficiency were calculated and listed in **Table 3**, which reveal that the inhibition efficiency ($\eta_p\%$) increases with increasing of the inhibitor concentration. The order of inhibition efficiency decreased as follows: III>II>I.

3.3. Electrochemical impedance measurements

The impedance measurements were carried out after immersion for 3 hours in the test solutions. **Figs 4, 5** show a typical set of Nyquist plots and Bode plots of compound III as a representative sample in the absence and presence of various concentrations. Various parameters such as, and percentage inhibition efficiency ($\eta_i\%$) were calculated according to the following equations and listed in **Table 4** [34]:

$$C_{dl} = [(1/2\pi f_{max})(1/R_{ct})] \quad (8)$$

$$\eta_i \% = [1 - (R_{ct} / R_{ct}(inh))] \times 100 \quad (9)$$

where R_{ct} and $R_{ct}(inh)$ are the charge transfer resistance values in the absence and presence of inhibitor, respectively. Increasing the value of charge transfer resistance (R_{ct}) and decreasing the value of double layer capacitance (C_{dl}) by increasing the inhibitor concentration indicate that the surfactant molecules inhibit corrosion rate of carbon steel in the test solution by adsorption mechanism [35]. For analysis of the obtained impedance spectra, the equivalent circuit (EC) was obtained using EIS analyzer as shown in **Fig. 6** where (R_s) is the solution resistance, (R_f) is the film resistance and (C_f) is the film capacitance. From the obtained results, it was found that the surfactant molecules inhibited the corrosion rate as indicated by increasing the value of charge transfer resistance (R_{ct}) and decreasing the value of double layer capacitance (C_{dl}) with increasing the inhibitor concentration, hence inhibiting the corrosion rate on carbon steel surface by adsorption mechanism [36]. It was found that the values of film resistance (R_f) were increased by increasing the inhibitor concentrations, while (C_f) values were decreased. This data conform the formation of a good

protective film of the inhibitor molecules on carbon steel surface.

3.4. Surface active properties measurements

The relationship between the surface tension and $-\ln C$ of the synthesized surfactants at 25 °C is shown in **Fig.7**. It is clear that the surface tension vs. $-\ln C$ relationship is characterized by two distinguishable regions. One at low concentration range and characterized by a fast decrease in the surface tension value, while at higher concentrations where the surface tension variation remains almost constant by increasing the concentration. The concentration at the break point of these two regions produces is taken as the critical micelle concentration (CMC). The CMC values were determined from the figure and listed in **Table 5**. It is obvious that the increase in hydrophobic chain length decreases the value of the CMC [37]. The organic character of the hydrophobic chains in the surfactant molecules increases the repulsion between these molecules and the aqueous phase. Also, hydrophobic moieties on the head group (Isopropyl and Toluene) in surfactant (II and III) respectively increase the repulsion between the surfactant molecules and the aqueous phase. Hence, the increase in repulsion between the surfactant molecules and the aqueous phase increases the tendency of the surfactant molecules toward adsorption at the air–water interface. That causes fast saturation of the interface by the adsorbed molecules. As a result, it is expected that increasing the hydrophobic chain length will increase the adsorption of the molecules at the interface and will also increase the tendency of the molecules toward micellization in the bulk of their solutions [38]. The maximum surface excess concentration (Γ_{max}) in mol/cm² was calculated from the following relationship [39]:

$$\Gamma_{max} = - (1/nRT) (dy/d \ln C) \quad (10)$$

where : T is absolute temperature, R is universal gas constant ($R = 8.314 \times 10^7$ ergs mol⁻¹ K⁻¹), and $dy/d \ln C$ is surface activity. The Γ_{max} values in Table 5 were used to calculate the average minimum area per adsorbed molecule at the aqueous–air interface at saturated condition (A_{min}) using the following relationship [39]:

$$A_{min} = 10^{16} / (N_A \cdot \Gamma_{max}) \quad (11)$$

where : N_A is “Avogadro’s number = 6.023×10^{23} molecule/mole”

3.5. Thermodynamic parameters of surface tension

The ability for micellization processes depends on the thermodynamic parameter (standard free energy, ΔG_{mic}). Most information on the free energy of micellization has been obtained indirectly through the CMC [40]. The ΔG_{mic} may be calculated by choosing the following expression equation (12):

$$\Delta G_{mic} = RT (1-\alpha) \ln CMC \quad (12)$$

where R is the universal gas constant ($R = 8.314$ J/mol.K), T is the absolute temperature, α is the fraction of counter ions bound by micelle in case of ionic surfactants ($\alpha=0$ for nonionic surfactants) and CMC is the critical micelle concentration in mol/L. Many investigations deal with the thermodynamics of surfactant adsorption at the interface [41]. The thermodynamic parameters value of adsorption ΔG_{ads} were calculated via the following equation (13):

$$\Delta G_{ads} = \Delta G_{mic} - 0.6023 \Pi_{CMC} A_{min} (13)$$

The free energy of micellization in **Table 5** indicates that the micellization process is spontaneous ($\Delta G_{mic} < 0$). The data show also that, the negativity of ΔG_{mic} for surfactants increased as follows (III > II > I) and this may be due to the effect of hydrophobic moieties on the head group. This behavior indicates that increasing the oxyethylene chain length favors the micellization process. From the data obtained, it was found that all ΔG_{ads} values are negative and they are more negative than ΔG_{mic} values. This indicates that, the adsorption at the interface is associated with a decrease in the free energy of the system i.e. the adsorption process is more spontaneous. Also, this indicates that, the studied surfactants favor adsorption than micellization.

3.6. Adsorption isotherm

To understand the corrosion inhibition mechanism, the organic compound's adsorption behavior on the carbon steel surface must be known. The plot of C_{inh}/θ vs. C_{inh} **Fig.8** yielded a straight line, provided that the adsorption of the synthesized surfactants from the deep oil well formation water obeys Langmuir adsorption isotherm, which is presented by equation (14) [42].

$$C_{inh}/\theta = 1/K_{ads} + C_{inh} \quad (14)$$

where C_{inh} is the inhibitor concentration and K_{ads} is the equilibrium constant for the adsorption/desorption process. From the intercepts of the straight lines on the C_{inh}/θ -axis, one can calculate K_{ads} , which is related to the standard free energy of adsorption, ΔG_{ads}^0 , as given by Eq. (15) [43]:

$$\Delta G_{ads}^0 = -RT \ln(55.5 K_{ads}) \quad (15)$$

The calculated free energy of adsorption (ΔG_{ads}^0) is given in **Table 6**. The negative values of ΔG_{ads}^0 indicated that the adsorption of the inhibitors on the metal surface is spontaneous. Generally, values of ΔG_{ads}^0 around -20 kJ mol^{-1} or lower are consistent with the electrostatic interaction between charged molecules and the charged metal surface (physisorption) [44]; those around -40 kJ mol^{-1} or higher involve charge sharing or transfer from organic molecules to the metal surface to form a coordinate type of metal bond (chemisorption) [42]. It can be seen from **Table 6** that, calculated ΔG_{ads}^0 values indicated that the adsorption mechanism of the prepared surfactants on carbon steel in the deep oil well formation water is (physical adsorption). The large values of ΔG_{ads}^0 and its negative sign are usually characteristic of strong interaction and a highly efficient adsorption.

3.7. Scanning electron microscopy (SEM)

Fig. 9a shows SEM image of polished carbon steel surface. The micrograph shows a characteristic inclusion, which was probably an oxide inclusion [45]. **Fig. 9b** shows SEM of the surface of carbon steel specimen after immersion in formation water for three days in absence of inhibitor, while **Fig. 9c** shows SEM of the surface of another carbon steel specimen after immersion in formation water for the same time interval in the presence of 500 ppm of the inhibitor (III). The resulting scanning electron micrographs reveal that, the surface was strongly damaged in the absence of the inhibitor, but in the presence of 500 ppm of the inhibitor (III), there is less damage in the surface. This confirms the observed high inhibition efficiency of the inhibitor (III) at this concentration.

3.8. Energy dispersive analysis of X-rays (EDX)

The EDX spectrum in **Fig. 10a** shows the characteristic peaks of some of the elements constituting the polished carbon steel surface. The spectrum of the polished carbon steel surface after immersion in the formation water in the absence and presence of inhibitor (III) for three days is shown in **Figs. 10b** and **10c** respectively. The spectrum of **Fig. 10c** shows that the Fe peak is considerably decreased relative to the samples in **Figs. 10a** and **10b**. This decreasing of the Fe band is indicated that strongly adherent protective film of inhibitor (III) formed on the polished carbon steel surface, which leads to a high degree of inhibition efficiency [46]. Therefore, the EDX and SEM examinations of the carbon steel surface support the results obtained from the chemical and electrochemical methods that the synthesized surfactant inhibitors are a good inhibitor for the carbon steel in the oil wells formation water.

3.9. Quantum chemical calculations

To investigate the relationship between molecular structure of these surfactants and their inhibition effect, quantum chemical calculations were performed. Geometric structures and electronic properties of (I, II and III) used as corrosion inhibitors were calculated by ab initio method with 3-21G** basis set. The optimized molecular structures and the frontier molecule orbital density distribution of the studied molecules are shown in **Fig.11**. Calculated quantum chemical indices E_{HOMO} , E_{LUMO} , ΔE , dipole moment are given in **Table 7**. For HOMO of the studied compounds, it can be observed that the increase in bond length makes distortion motion in the solution which increases the free energy (ΔG). For I and II the geometric structure of these inhibitors is tri angle look like structure which make good inhibition efficiency. It can be observed that for III (built on aromatic alkyl halide) the benzene ring, has larger electric density coming from the pz orbital of Π bond. Low values of the dipole moment will favor the accumulation of inhibitor molecules on the metallic surface. The lowest value of dipole moment was obtained by I(3.45), II(8.052) and III (8.058). These inhibitors exhibit the maximum inhibition efficiency (see **Table 3**). The HOMO–LUMO gap, i.e., the difference in energy between the HOMO and LUMO, is an important stability index [47]. We can mention the energy of the HOMO, which is often associated with the capacity of a molecule to donate electrons. Therefore, an increase in the values of HOMO can facilitate the adsorption and therefore the inhibition efficiency, by indicating the disposition of the molecule to donate orbital electrons to an appropriate acceptor with empty molecular orbitals. In the same way low values of the energy gap $\Delta E = E_{HOMO} - E_{LUMO}$ will render good inhibition efficiencies, because the energy needed to remove an electron from the last occupied orbital will be low [48, 49]. It has been reported in the literature that the higher the HOMO energy of the inhibitor, the greater the trend of offering electrons to unoccupied d orbital of the metal, and the higher the corrosion inhibition efficiency. In addition, the lower the LUMO energy, the easier the acceptance of electrons from metal surface, as the LUMO–HOMO energy gap decreased and the efficiency of inhibitor improved. The data of HOMO and LUMO for our inhibitors are listed in **Table 7**. Regarding from ΔE it was found that the minimum value obtained by which has the best inhibition efficiency.

4. Conclusion

The conclusion of this work can be stated in the following points:

- 1) Three surfactants based on N,N'-(azanediylbis(ethane-2,1-diyl))dioleamide which named (I, II, and III) were synthesized and purified. The chemical structure of these compounds was confirmed by ¹H NMR and FT-IR, and their surface properties were determined.
- 2) The prepared surfactants were examined as corrosion inhibitors. From all measurements performed, the prepared surfactants are good inhibitors for the corrosion of carbon steel in formation water. High inhibition efficiencies are observed around their CMCs, and the inhibition efficiency increases with increasing of inhibitor concentrations. The order of inhibition efficiency decreased as follows III>II>I.
- 3) Aromatic alkyl halide is the optimum to get the quaternary ammonium salts and have good inhibition efficiency.
- 4) The potentiodynamic polarization curves indicated that the inhibitors inhibit both anodic metal dissolution and cathodic hydrogen evolution reactions and acted as mixed type inhibitors in the test solution.
- 5) The adsorption of the inhibitors molecules on the metal surface from the test solution obeys Langmuir's adsorption isotherm. The adsorption process is spontaneous and act as physical adsorption.
- 6) Data obtained from quantum chemical calculations were correlated with the experimentally obtained inhibition efficiencies.
- 7) Quantum chemical calculations revealed that the adsorption of the three inhibitors was mainly concentrated around the nitrogen and oxygen atoms.

References

- [1] K. E. Heusler, D. Landolt, S. Trasatti, Journal of Electroanalytical Chemistry, 274 (1989)345.
- [2] S. Ghareba, S. Omanovic, Corrosion Science 52 (2010) 2104.
- [3] M. A. Hegazy, M. Abdallah, H. Ahmed, Corrosion Science 52 (2010)2897.
- [4] A. Hernández-Espejel, M.A. Domínguez-Crespo, R. Cabrera-Sierra, C. Rodríguez-Meneses, E. M. Arce-Estrada, Corrosion Science 52(2010) 2258.
- [5] M. A. Migahed, Progress in Organic Coatings 54 (2005) 91.
- [6] B. Brown, S. R. Parakala, S. Nesci, NACE International Corrosion Conference and Expo, 2004.
- [7] D. W. Shoesmith, P. Taylor, M. G. Bailey, D. G. Owen, Journal of Electrochemical Society. 127 (1980) 1007.
- [8] E. L. Hibner, B. Puckett, Corrosion(2003), NACE: Houston, TX, Paper No. 03125.
- [9] F. N. Speller, Corrosion Causes and Prevention, McGraw-Hill, New York, 1951.
- [10] A. Y. Musa, A. H. Kadhum, A. Mohamad, M. S. Takriff, Corrosion Science 52 (2010) 3331.
- [11] N. Kovac'evic', A. Kokalj, Corrosion Science 53 (2011) 909.
- [12] S. Ghareba, S. Omanovic, Electrochimica Acta 56 (2011) 3890.
- [13] V. S. Sastri, Corrosion Inhibitors—Principles and Applications, Wiley, Chichester, 1998.
- [14] I. B. Obot, S. A. Umoren, N. O. Obi-Egbedi, Journal of Material and Environmental Science 2(2011) 60.
- [15] M. A. Migahed, A. M. Al-Sabagh, E. G. Zaki, H. A. Mostafa and A. S. Fouda. Elixir Corrosion & Dye 77 (2014) 28958.
- [16] A. Ouchrif, M. Zegmout, B. Hammouti, A. Dafali, M. Benkaddour, A. Ramdani, S. Elkadiri, Progress in Organic Coating 53 (2005) 292.
- [17] L. J. Berchmans, S. V. K. Iyer, V. Sivan, Material Chemistry and Physics 98 (2006) 395.
- [18] D. N. Sing, A. K. Dey, Corrosion 49 (1993) 594.
- [19] G. Banerjee, S. N. Mahotra, Corrosion 48 (1992) 10.
- [20] S. T. Arab, E. A. Noor, Corrosion 49 (1993) 122.
- [21] L. A. Raspi, Nickel Corrosion 49 (1993) 821.
- [22] Y. Chen, Y. Wang, G. Zhang, Daily Chem. Ind. 2 (1986) 56.
- [23] L. Shi, H. Song, Daily Chem. Ind. 1 (1987) 9.
- [24] A. M. A. Omar, A. M. Sabagh, M. M. Osman, Material Chemistry and Physics 50 (1997) 271.
- [25] F. Bentiss, M. Lagrenee, M. Traisnel, Corrosion Science 42 (2000)127.
- [26] A. R. G. Isabel, M. A. B. Christopher, P. S. M. Jenny, Corrosion Science 36 (1994) 915.
- [27] C. Og'retir, E. Hur, G. Bereket, Journal of Molecular Structure 578 (2002) 79.
- [28] B. Mihci, C. Og'retir, G. Bereket, Journal of Molecular Structure 488 (1999)223.
- [29] P. R. Herrington, W. Yinqiu, Journal of the American Oil Chemists' Society 74 (1997)1.
- [30] Y. Ohshiro, M. Ochiai, and S. Komori, Journal of Electrochemical Society 64(1961)114.
- [31] A. M. Al-Sabagh, M. A. Migahed and H. S. Awad, Corrosion Science 48(2006)813.
- [32] R. G. Andrew, M. M. Michael, M. P. Rama, Journal of Dispersion Science and Technology 27 (2006) 731.
- [33] Q. B. Zhang, Y.X. Hua, Electrochimica Acta 54 (2009) 1881.
- [34] A. P. Yadav, A. Nishikata, T. Tsuru, Corrosion Science 46 (2004) 169.
- [35] K. F. Khaled, Applied Surface Science 252 (2006) 4120.
- [36] M. A. Migahed, M. M. Attia, M. Abd El-raouf, E. Khamis T. A. Ali and A. M. Al-Sabagh, International Journal of Electrochemical Science 10 (2015) 1343.
- [37] R. Oda, I. Huch, J. Sauveur, Chemical Communications 56 (1997) 2105.
- [38] N. A. Negm, Journal of Surfactants and Detergent 10 (2007) 87.
- [39] S. M. Hamid and D.C. Sherrington, Journal of British Polymer 16(1984) 39.
- [40] M. J. Rosen, Surfactants and Interfacial Phenomena, John Wiley and Son Inc., New York, 2004.

- [41] A. M. Al-Sabagh, D. R. K. Harding, N. G. Kandile, A. M. Badawi, Amira E. El-Tabey, Journal of Dispersion Science and Technology 30 (2009)472.
- [42] E. Cano, J. L. Polo, A. La Iglesia, J. M. Bastidas, Adsorption 10(2004) 219.
- [43] G. Quartarone, M. Battilana, L. Bonaldo, T. Tortato, Corrosion Science 50 (2008) 3467.
- [44] B. G. Ateya, B. E. El-Anadouli, F. M. A. El-Nizamy, Corrosion Science 24 (1984) 497.
- [45] ASTM E 45-87, vol. 11, ASTM, Philadelphia, PA, (1980) 125.
- [46] M.A. Amin, Journal of Applied Electrochemistry 36 (2006) 215.
- [47] D.F.V. Lewis, C. Ioannides, D.V. Parke, Xenobiotica 24 (1994)401.
- [48] N. Khalil, Electrochemica Acta 48 (2003) 2635.
- [49] P. Molymoux, C.T. Rhodes, J. Swarbrick, Transactions of the Faraday Society61 (1965) 1043.

List of Tables

Table 1: Chemical composition of carbon steel alloy (X70).

Element	C	Si	Mn	P	S	Ni	Cr	Mo	Cu	V , Nb ,Ti	Fe
Content (Wt. %)	0.07	0.3	1.15	0.008	0.001	0.01	0.2	0.01	0.02	Appropriate content	Rest

Table 2: Chemical composition and physical properties of deep oil well formation water used in this investigation

Property	Unit	Value
Density	g/cm ³	1.206
Salinity as NaCl	ppm	303567
Resistivity	Ω.m	0.017
PH		6.38
Ionic species	Value(ppm)	
Sulfate	600	
Chloride	183980	
Sodium	43760	
Iron	683	
Strontium	94	
Calcium	57720	
Magnesium	12	
Barium	7	
Lead	372	
Potassium	10930	
Zinc	374	

Table 3: Data obtained from potentiodynamic polarization measurements of carbon steel X70 immersed in deep oil well formation water in the absence and presence of various concentrations of the inhibitors (I, II and III) at 298K

Inhibitor	Conc. (ppm)	E _{corr} (mV)	I _{corr} , (μAcm ²)	β _c (mV)	β _a (mV)	R _p (kΩcm ²)	θ	η _p (%)
Formation water (blank)	-	-602.2	223	-169.1	105.1	0.26	-	-
	100	-641.9	132	-132.8	119.1	0.33	0.408	40.8
	200	-602.6	87.4	-196.9	213.8	0.46	0.608	60.8
	300	-699.5	69.5	-184.5	140.2	0.51	0.688	68.8
	400	-715.2	60.4	-189.7	150.1	0.66	0.729	72.9
	500	-718	55	-163.3	111.2	0.55	0.753	75.3
Inhibitor II	100	-664.2	110.8	-188.6	139.7	0.33	0.503	50.3
	200	-678.6	84.7	-274.6	165.8	0.7	0.62	62
	300	-682	68.9	-254.8	162.1	0.82	0.691	69.1
	400	-673.1	59.9	-184.2	147.7	0.61	0.731	73.1
	500	-669.4	54.2	-262.8	174.5	0.8	0.757	75.7
Inhibitor III	100	-685.2	100.1	-232.5	184.3	0.5	0.551	55.1
	200	-684	82.8	-153	113.7	0.34	0.629	62.9
	300	-659.7	68.9	-209.6	185.1	0.67	0.691	69.1
	400	-718.8	60	-190	141	0.58	0.731	73.1
	500	-666	50.4	-205.7	151.9	0.97	0.774	77.4

Table 4: Data obtained from electrochemical impedance spectroscopy (EIS) measurements of carbon steel in the test solution in the absence and presence of various concentrations of the inhibitors (I, II and III) at 298K.

Inhibitor	Conc. (ppm)	R_s ($\Omega \text{ cm}^2$)	C_r ($\Omega^{-1} \text{ s}^n \text{ cm}^2$)	n	R_r ($\Omega \text{ cm}^2$)	C_{dl} ($\Omega^{-1} \text{ s}^n \text{ cm}^2$)	n	R_{ct} ($\Omega \text{ cm}^2$)	η_i (%)
Formation water (blank)	-	3.9	2.4	0.8	13.17	16.41	0.8	166.4	-
Inhibitor I	100	4.52	4.5	0.9	18.6	16	0.59	285.04	41.62
	200	6.23	8.7	0.82	20.87	21	0.54	355.41	53.18
	300	5.27	4.7	0.88	19.67	32	0.47	393.97	57.76
	400	5.97	19.9	0.69	44.24	14	0.55	437.39	61.96
	500	6.25	13.3	0.73	43.54	14	0.62	538.08	69.07
Inhibitor II	100	4.49	13.9	0.78	36.99	21.08	0.53	316.55	47.43
	200	4.48	9.72	0.82	26.59	16	0.6	365.23	54.44
	300	5.35	16.7	0.79	24.38	18.53	0.52	401.36	58.54
	400	5.41	14.7	0.82	21.71	15.76	0.52	438.62	62.06
	500	4.98	13.3	0.79	28.57	14.19	0.56	544.54	69.44
Inhibitor III	100	6.07	10.2	0.8	29.06	18.87	0.61	326.43	49.02
	200	5.3	20.1	0.82	46.39	18.04	0.51	366.97	54.66
	300	4.77	27.3	0.68	59.66	17.03	0.52	403.27	58.74
	400	5.08	2.73	0.85	12.85	27.36	0.83	442.85	62.43
	500	4.59	8.17	0.82	19.33	22.8	0.51	584.85	71.55

Table 5: Surface active properties of the investigated surfactants at 298K.

Inhibitors	$\text{CMC} \times 10^{-4}$ (mol L^{-1})	γ_{CMC} (mNm^{-1})	π_{CMC} (mNm^{-1})	$\Gamma_{\text{Max}} \times 10^{10}$ (mol cm^{-2})	A_{min} (\AA^2)	ΔG_{mic} (kJ mol^{-1})	ΔG_{ads} (kJ mol^{-1})
I	4.1	41.3	31	1.53	108.83	-19.30	-21.33
II	3.8	40.65	31.65	1.57	106.03	-19.50	-21.54
III	3.7	39.33	32.97	1.60	103.88	-19.57	-21.63

Table 6: Adsorption parameter of three inhibitors on carbon steel in test solution at 298K

Inhibitors	R^2	$K_{\text{ads}} \times 10^4 (\text{M}^{-1})$
I	0.997	1.19
II	0.999	1.85
III	0.997	2.16

Table 7: Calculated quantum chemical parameters of studied inhibitors.

Compound name	$E_{\text{HOMO}}(\text{eV})$	$E_{\text{LUMO}}(\text{eV})$	$\Delta E(\text{eV})$	$\mu(\text{debye})$	LogP	The number of transferred electrons, ΔN
I	-8.00	0.788	8.788	3.45	8.34	0.386
II	-9.741	0.217	9.958	8.052	10.09	0.224
III	-2.238	0.203	2.441	8.058	11.46	0.213

*The theoretical values of absolute electronegativity of iron (X_{Fe}), the absolute hardness of iron (η_{Fe}) and the electronic chemical potential of iron (μ_{Fe}) are 7, 0 and -7 eV/mol, respectively

List of figures

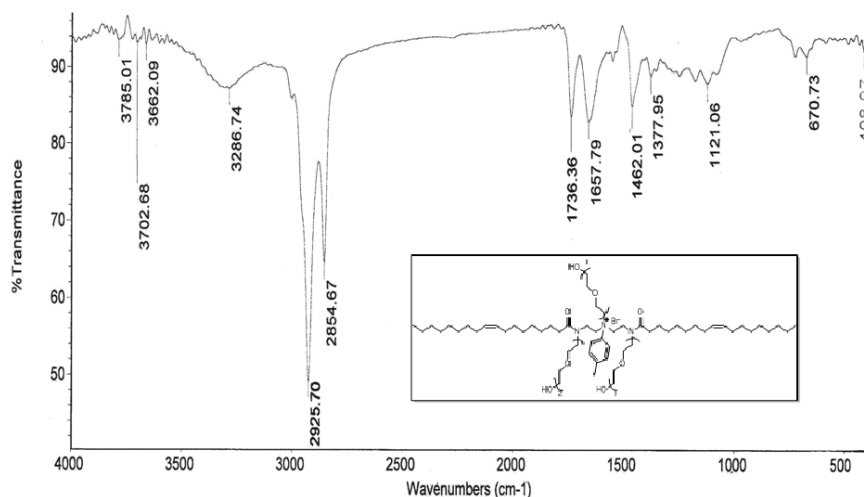


Figure 1: FTIR spectrum of inhibitor (III).

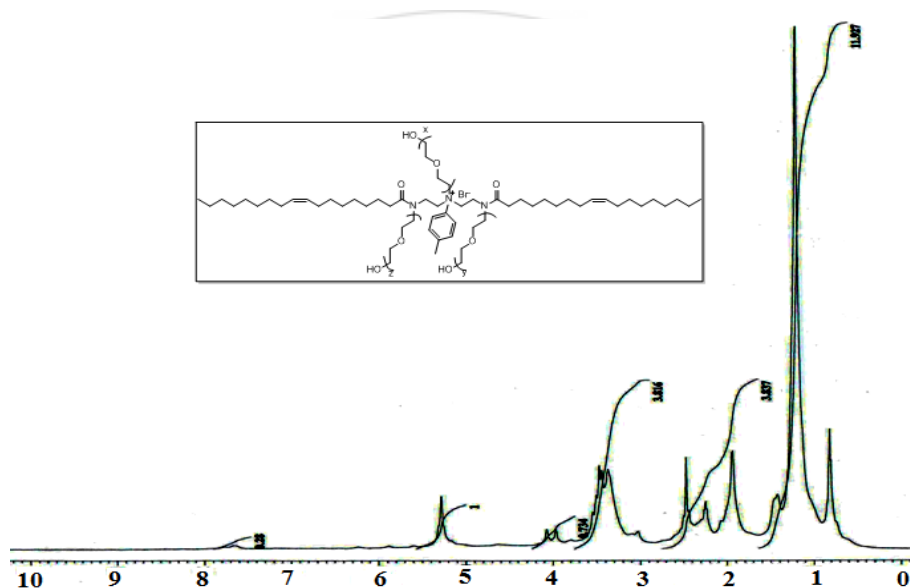


Figure 2: ¹H NMR spectrum of inhibitor (III).

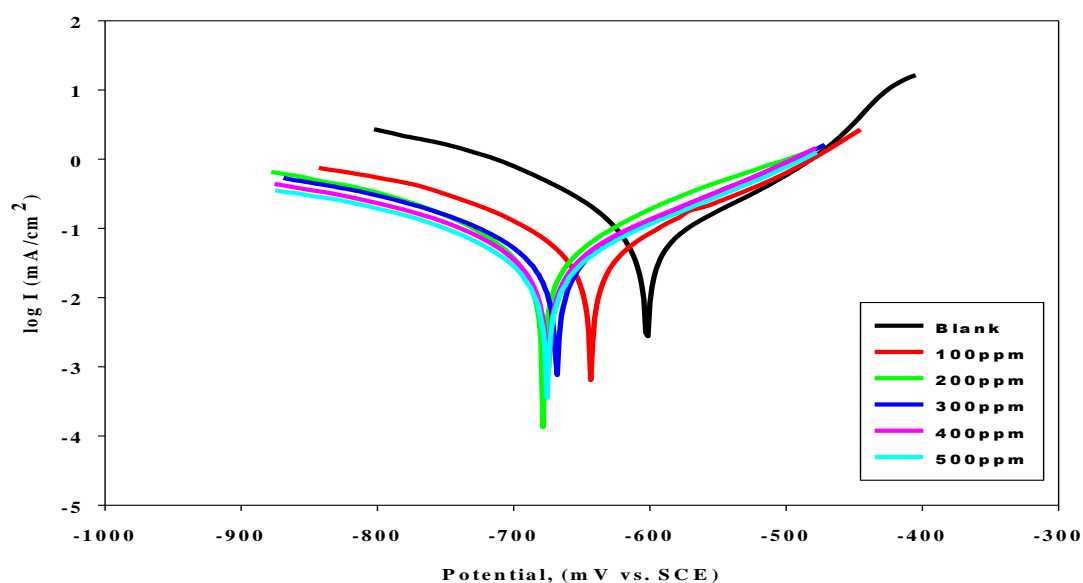


Figure 3: Potentiodynamic polarization curves of carbon steel in the test solution in the absence and presence of different concentrations of inhibitor (III) at 298K.

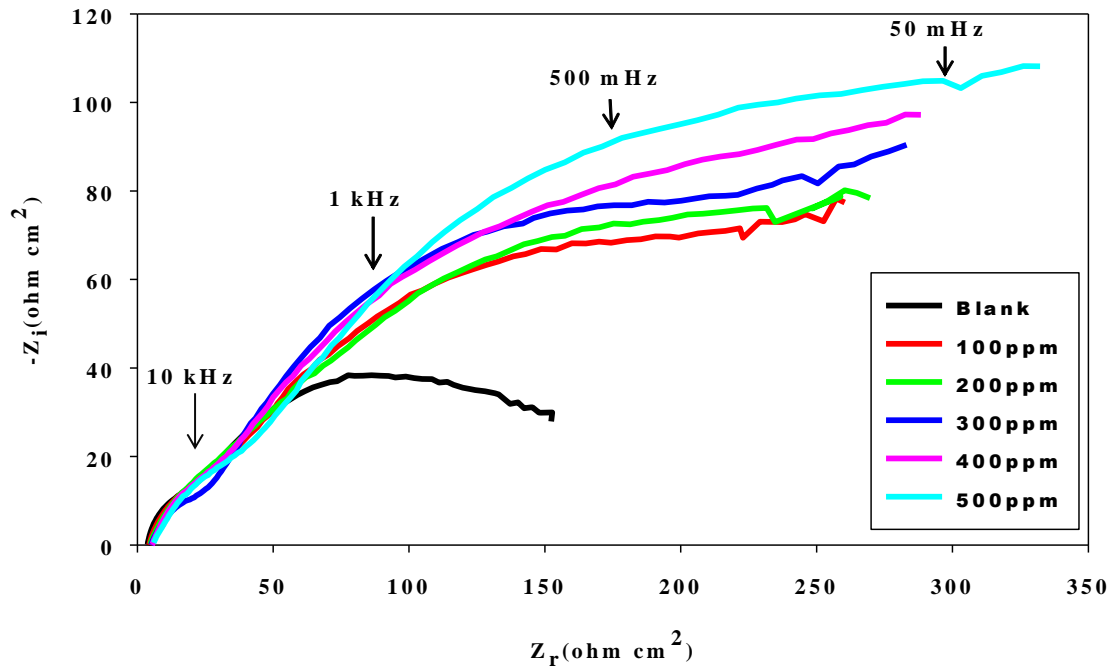


Figure 4: Nyquist plots for carbon steel in the test solution in the absence and presence of different concentrations of inhibitor (III).

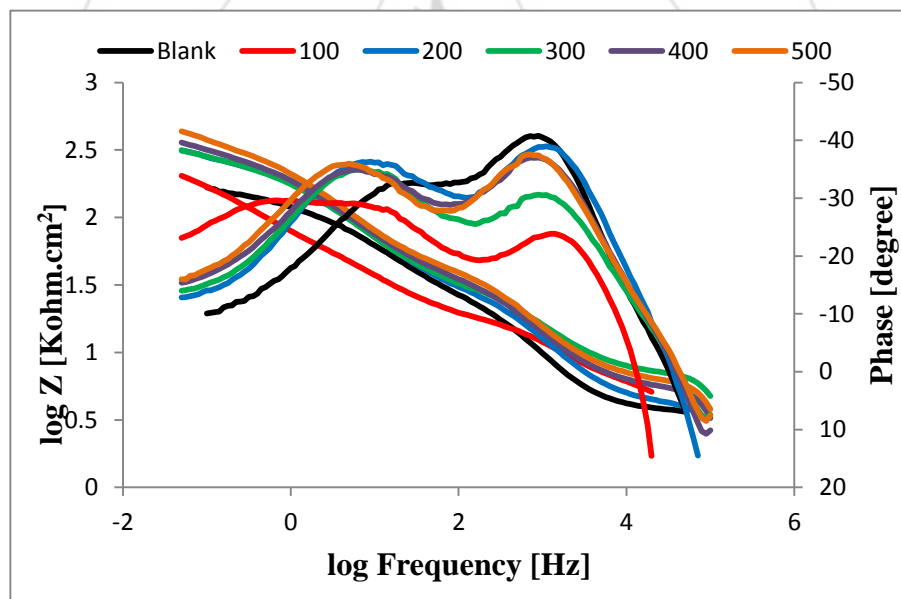


Figure 5: Bode plots for the carbon steel in the test solution in the absence and presence of various concentrations of inhibitor (III).

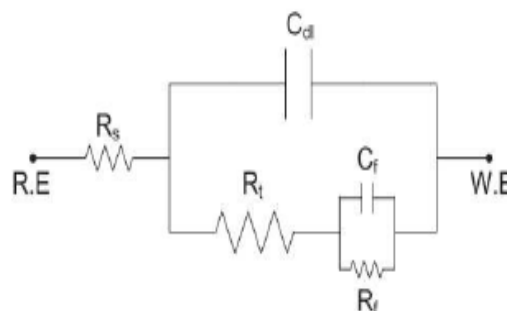


Figure 6: Equivalent circuit used to model impedance data of carbon steel in oil well formation water under CO_2 and H_2S environments.

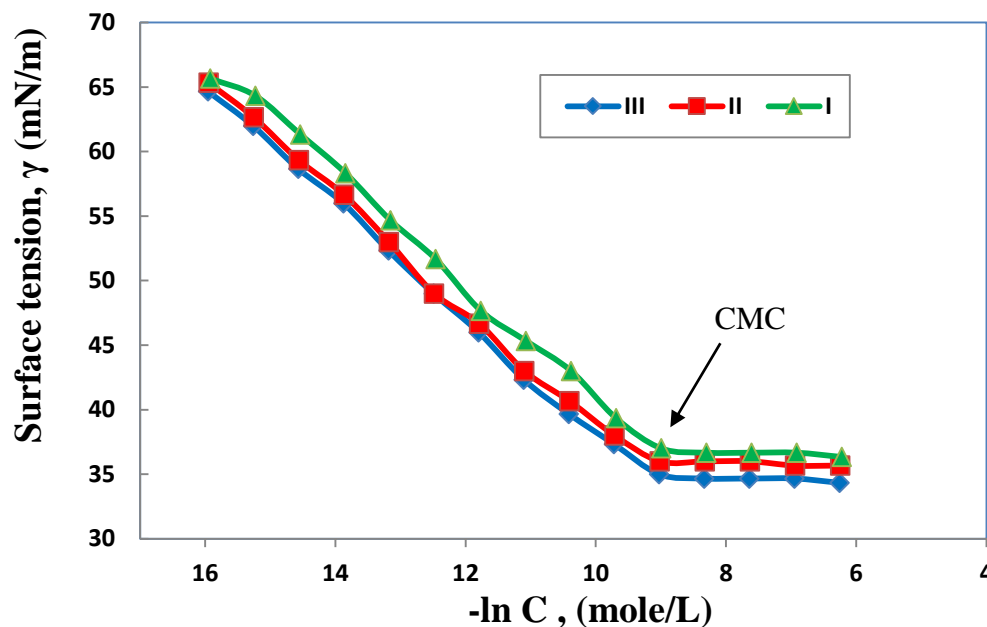


Figure 7: Surface tension (γ) vs. log C at different concentrations of the inhibitor (I, II and III) at 298K.

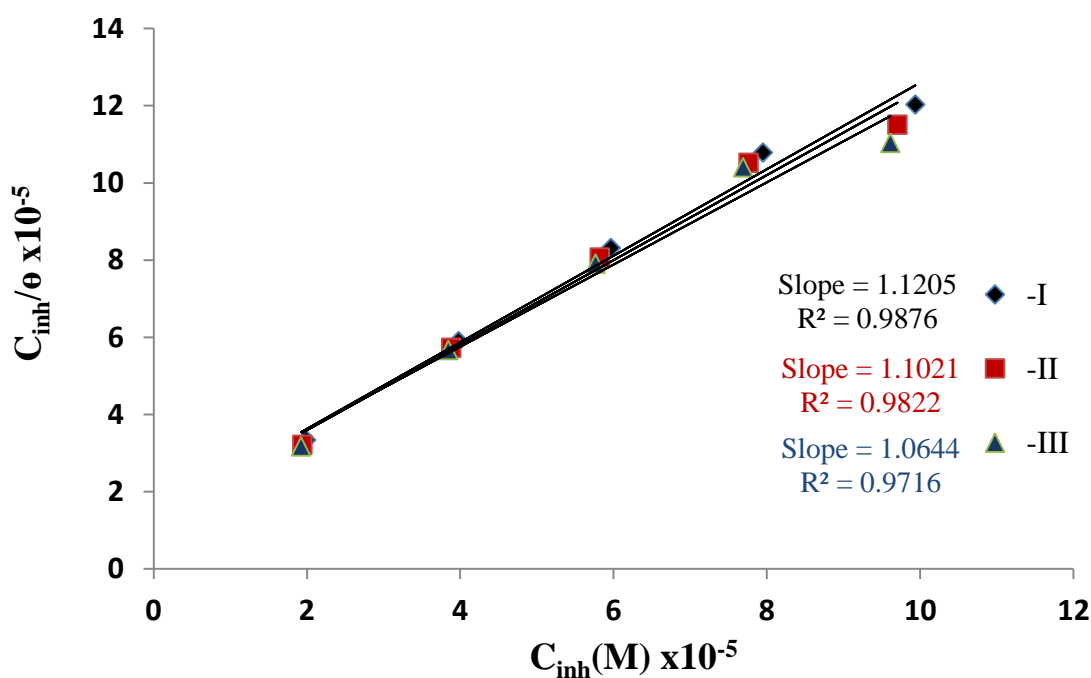


Figure 8: Langmuir isotherms for the adsorption of the prepared surfactants on carbon steel surface in test solution at 298K.

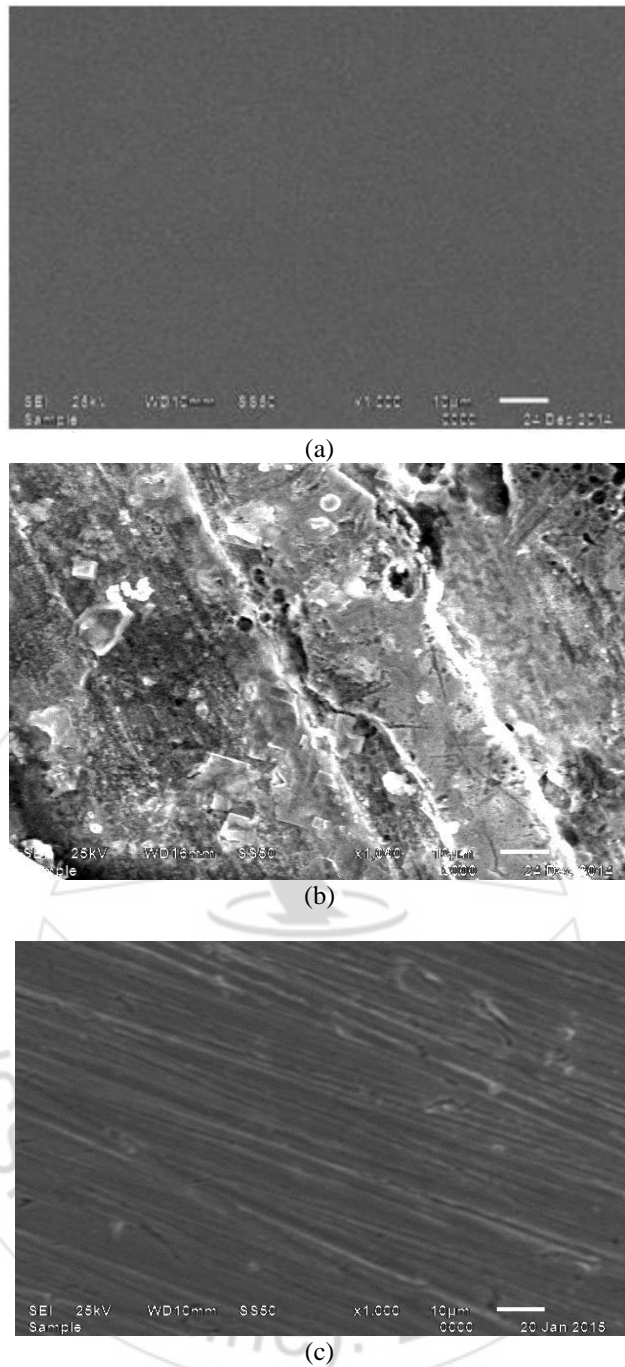


Figure 9: SEM of the carbon steel surface: (a) polished sample, (b) after immersion in the formation water and (c) after immersion in the formation water in the presence of 500 ppm of compound III

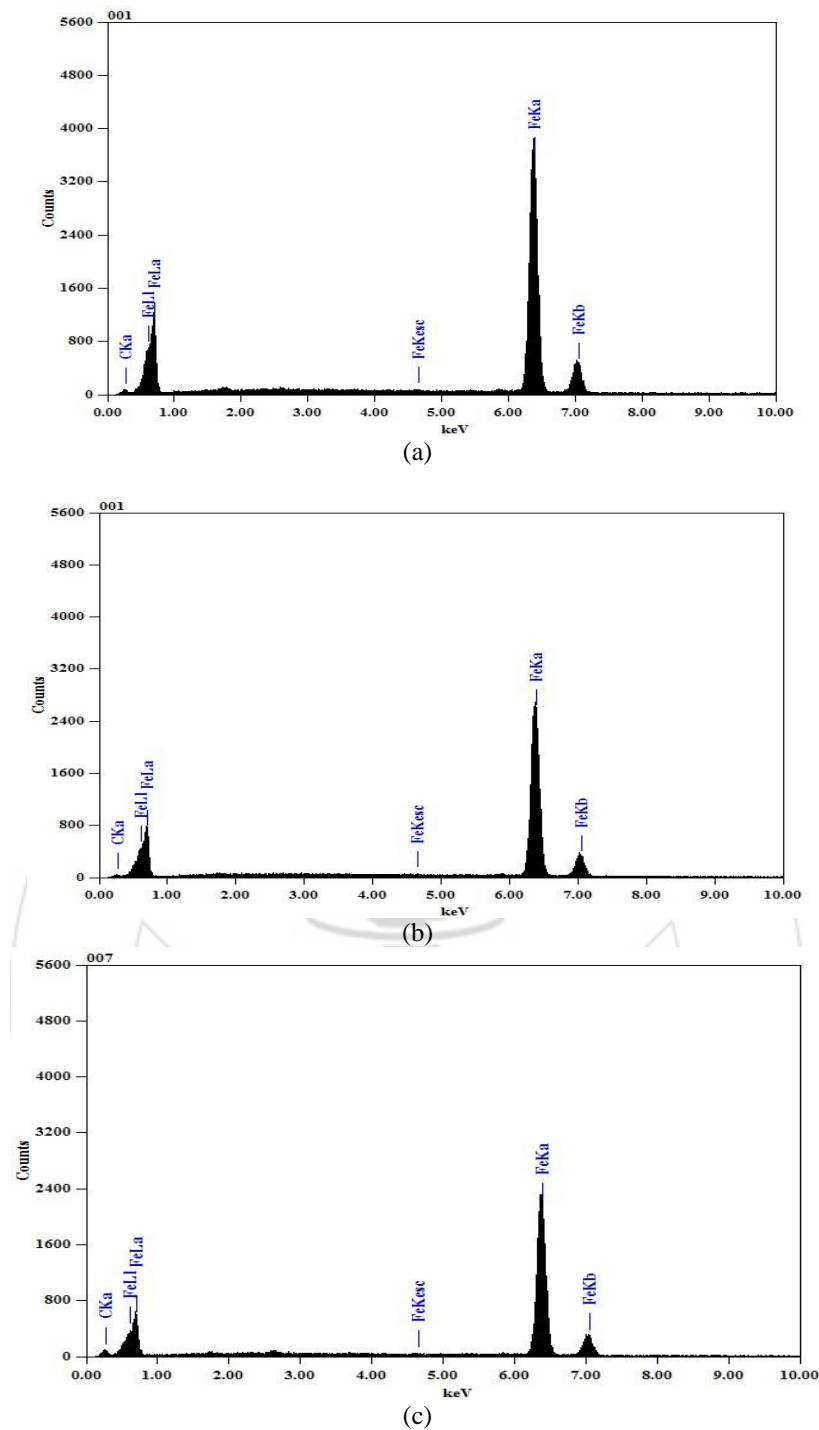


Figure 10: EDX of the carbon steel surface: (a) polished sample, (b) after immersion in the formation water and (c) after immersion in the formation water in the presence of 500 ppm of inhibitor (III).

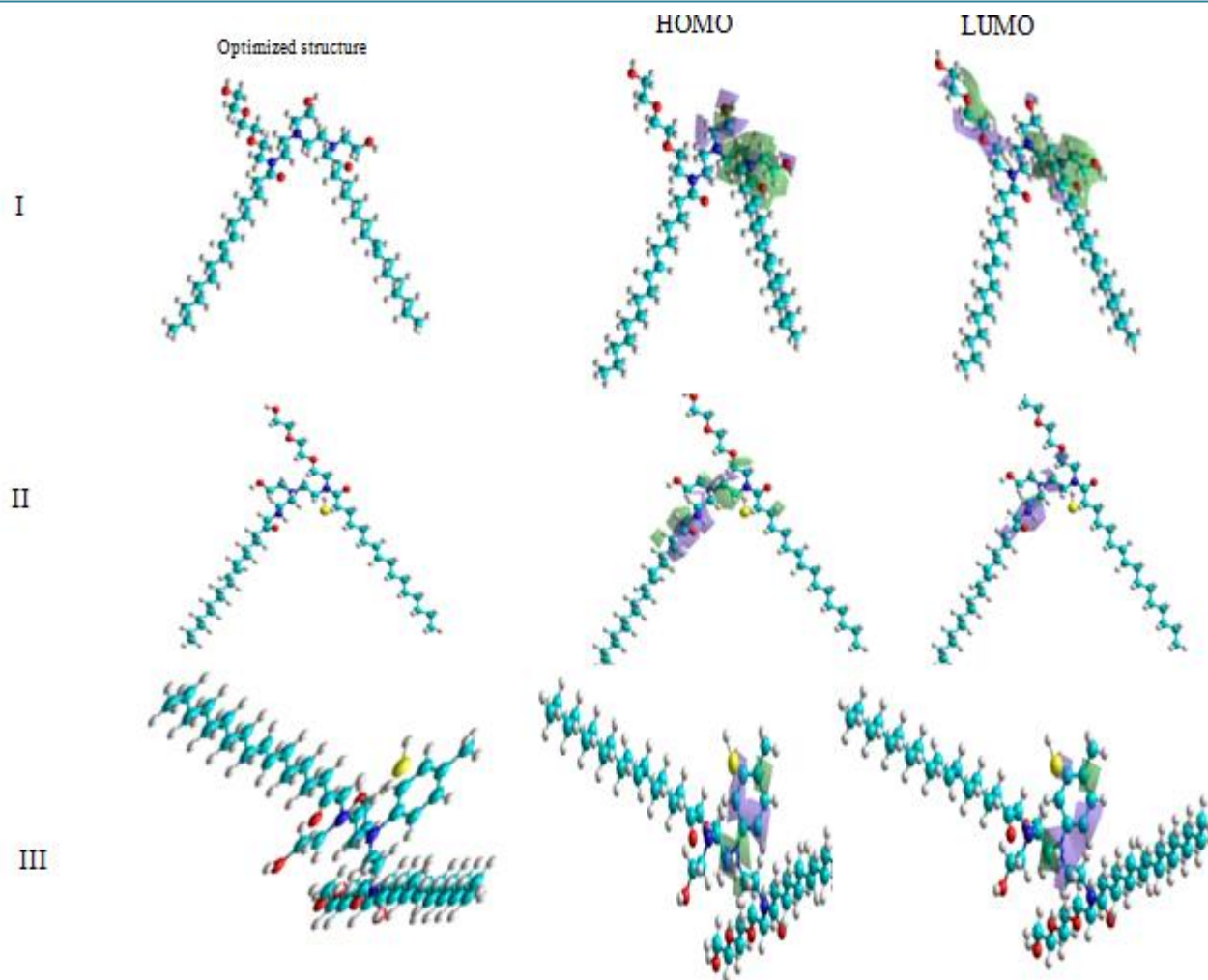


Figure 11: Molecular structure and HOMO–LUMO of compounds I,II and III.